A novel concept for managing thermal interference between geothermal systems in cities

Guillaume Attard, Peter Bayer, Yvan Rossier, Philipp Blum, Laurent Eisenlohr

A novel concept for managing thermal interference between geothermal systems in cities

Guillaume ATTARD[1]*, Peter BAYER[2], Yvan ROSSIER[3], Philipp BLUM[4], Laurent EISENLOHR[1]

[1] Cerema, Direction Centre-Est, 46 rue Saint Théobald, F-38081 L'Isle d'Abeau, France

[2] Ingolstadt University of Applied Sciences, Institute for new Energy Systems (InES), Esplanade 10, 85049 Ingolstadt, Germany

[3] Univ. Grenoble Alpes, Institut des Géosciences de l'environnement (IGE), Domaine universitaire, 1381 rue de la piscine, F-38400 Saint Martin d'Hères, France

[4] Karlsruhe Institute of Technology (KIT), Institute of Applied Geosciences (AGW), Kaiserstraße 12, 76131 Karlsruhe, Germany

*Corresponding author: Guillaume ATTARD, Guillaume.attard@cerema.fr

Abstract

The growing interest in shallow geothermal resources leads to dense installation areas, where interference and decrease in efficiency might occur. To optimize geothermal use in cities which prevents interference between neighbouring and future installations, we present a novel concept relying on the definition of thermal protection perimeters (TPP) around geothermal installations. These perimeters are determined by quantifying the thermal probability of capture around closed- and open-loop geothermal systems. Then, the maximal acceptable power that can be exploited in the vicinity of the installations can be continuously mapped. Existing analytical heat transport models are adapted to calculate these thermal capture probabilities. Two applications are illustrated in Lyon (France). The first application shows that adapted analytical models can help to manage multiple geothermal installations already in place in sectors of few square kilometres. In the second application, a numerical deterministic model is used to determine the TPP of one open-loop system at a local scale. The numerical approach applied for this case allows to account for flow disturbances caused by underground constructions, and thus offers a refined representativeness of the probability of capture. The presented methodology facilitates compatibility assessments between existing and planned new geothermal installations, which is otherwise not feasible by only mapping thermal plumes caused by existing installations, as done in common practice.

Highlights

- A novel methodology to manage multiple geothermal installations is presented.
- This methodology is based on the delineation of capture zones.
- Two analytical models are adapted to determine thermal probabilities of capture.
- A numerical model is used to apply the methodology in a densely built environment.

Keywords

Shallow geothermal energy; thermal impact; groundwater; analytical solutions; numerical modelling

Nomenclature table

Symbol	Variable	Unit
b	Thickness of aquifer	[m]
$BMAP$	Background maximal acceptable power	[W]
C	Volumetric heat capacity	[J Kg^{-1} K^{-1}]
D	Hydrodynamic dispersion coefficient	[m^2 s^{-1}]
F_o	Energy injection per length of borehole	[W m^{-1}]
F_{PTA}	Heat flow through protection target area	[W]
g	Transfer function	[-]
i	Hydraulic gradient	[-]
I	External power	[W]
K	Hydraulic conductivity	[m s^{-1}]
MAP	Maximal acceptable power	[W]
n	Porosity	[-]
p	Probability	[-]
q_h	Injected heat power	[W]
Q_p	Injection/pumping rate	[m^3 s^{-1}]
t	Time	[s]
T	Calculated temperature	[K]
T_{inj}	Temperature of injected water	[K]
T_a	Undisturbed temperature of aquifer	[K]
T_p	Temperature at the production well (open system)	[K]
ΔT_{inj}	Temperature difference between T_{inj} and T_a	[K]
ΔT	Temperature difference between T and T_a	[K]
ΔT_o	Temperature difference at injection point	[K]
ΔT_{max}	Maximal temperature alteration	[K]
v_a	Seepage velocity	[m s^{-1}]
x	x-coordinate	[m]
y	y-coordinate	[m]
Y	Dimension of planar source in y-direction	[m]
α	Dispersivity	[m]
λ	Thermal conductivity	[W m^{-1} K^{-1}]
Subscripts		
BHE	Individual borehole	
cl	Closed-loop geothermal installation	
op	Open-loop geothermal installation	
up	Upstream	
dw	Downstream	
k	Installation or borehole index	
w	Water	
s	Soil	
m	Porous media	
L	Longitudinal	
T	Transverse	

1 Introduction

There is an increasing interest in utilizing shallow ground and groundwater as a source for geothermal heating and cooling [1-4]. Either open- or closed-loop systems can be used for heat exchange with the subsurface to supply heat pumps of buildings. Open-loop systems are either single or groups of wells which utilize groundwater directly as a heat carrier. Commonly, such groundwater heat pump (GWHP) systems are installations of doublet configurations with an extraction well for groundwater abstraction, and an injection well, where water is injected back into the same aquifer at the same rate, but at an altered temperature [5, 6]. Standard closed-loop systems consist of vertical boreholes (BHEs) where plastic tubes are installed for circulating a heat carrier fluid. Such ground source heat pump (GSHP) systems are implemented with single or multiple vertical BHEs depending on the heat demand that must be supplied [7].

Augmented geothermal utilization entails a higher density of installations and potential competition among adjacent systems. This raises the need for management of neighbouring installations that may interfere with each other [8-13]. Interference means that the thermal impact of one system is not only measurable as local temperature anomaly in the ground, but it also influences the performance of another system in the vicinity. When neighbouring geothermal installations are regularly operated in a similar mode of seasonal heating and cooling, there is a risk that thermal interference mitigates the technological performance [14-17]. Thus, for concerted management of dense installations, especially in cities, authorities and operators have to account for potential thermal interference. Proper management of these systems, however, is not only required in order to regulate the competition for the limited geothermal resource, but is also particularly relevant for sustainable thermal groundwater management that prevents heating or cooling of the subsurface towards environmentally critical levels [18, 19].

In the scientific literature, there have been several concepts presented to support spatial planning and management of co-existing geothermal applications. A common procedure is the application of (semi-) analytical [15, 20, 21] or numerical models [12, 22-26] to describe the thermal stress of urban aquifers. Analytical models are commonly based on superpositioning of line-source models that allow straightforward simulation of multiple interacting BHEs of closed-loop systems [27-30]. Single GWHP systems can also be simulated by analytical models [6, 13, 31], but especially when the focus is on interference among neighbouring and larger systems, numerical models are commonly favoured [12, 32-34].

Available concepts set the focus on deterministic simulation. Aside from this, thermal impact is often quantified by arbitrary temperature thresholds in order to delineate thermal plumes and/or so-called "thermally affected zones" (TAZ) [20, 35-37]. A common practice is to map thermal plumes caused by existing installations to guide positioning of new installations outside of these TAZ. This, however, may be misleading, as beyond such theoretical plume boundaries geothermal systems also have thermal impact. Consequently, beyond these boundaries, there may exist thermal interference among neighbouring installations. As a solution, a very narrow threshold could be chosen. In this case, the theoretical plume extensions become enormous as a consequence of lateral heat diffusion described by Fourier's law. This would be unreasonable and prohibitive for any new geothermal installations, despite only marginal interference. In view of this, there is obviously a need for alternative criteria rather than relying only on a fixed temperature threshold. However, a temperature threshold is a convenient criterion that can be easily understood, measured and applied. Ideally, we can refer to a certain temperature threshold depending on thermal performance ranges of geothermal devices, but we should also interpret its relation to hydro-thermal interference in terms of competitive geothermal energy use of neighbouring systems.

In this study, a novel methodology to quantify and prevent thermal interference is presented. The aim of this methodology is to define the appropriate distance that should be kept between existing and future installations of different power to protect existing installations and optimally manage the urban thermal use of shallow groundwater. The following section introduces how thermal capture probability can be used as a criterion to define protection perimeters around geothermal installations. Subsequently, analytical models are adapted to calculate thermal capture probabilities, as well as the maximal acceptable power that can be exploited by open- and closed-loop geothermal installations. These analytical as well as numerical simulations are subsequently applied to two case studies. The first one illustrates how adapted analytical models can help to manage multiple open geothermal installations on a district scale. The second application shows how numerical models can be used to quantify thermal capture probability around a geothermal installation on the scale of a project, where groundwater flow is disturbed by several underground constructions.

2 Definition of a thermal protection perimeter

The problem we are studying is to define a thermal protection perimeter around a geothermal installation to avoid an unreasonable temperature alteration (ΔT_{max}), which would be caused by an external heat injection I (Fig. 1). By "unreasonable" we refer to any unwanted, threatening, technically critical or illegal temperature alteration. The following definitions are given:

- The **protection target area** (PTA) of a geothermal installation is defined as the small core area that includes all heat production devices of the installation.
- The **thermal protection perimeter** (TPP) of an installation is defined as the surrounding area, where an external heat injection I generates a temperature alteration above ΔT_{max} in the protection target area of the installation.

The interaction between the external heat injection and the PTA can be described by a transfer function, which is defined as the outlet response of the advective-dispersive system to a heat Dirac input at the location of the external heat injection. This transfer function represents a probability density function of travel time distribution between the external heat injection location and the PTA. This concept is commonly used to define protection perimeters around water supply wells that are prone to contamination [38-41]. For further details on mathematical techniques for obtaining transfer functions in hydrogeology, readers are referred to [42, 43]. Based on the analogy between the advection-dispersion equation for solute and heat transport, this was adopted by Milnes and Perrochet [44] to assess the impact of thermal feedback and recycling within single geothermal well doublets. A similar approach is proposed here, but the new idea is for separately operating potentially competitive neighbouring systems.

Given a transfer function $g(t)$ between the location of an external heat injection and the PTA, the probability $p(t)$ that a heat quantity introduced into the aquifer at the injection location is captured at the PTA at a time t is obtained by

$$p(t) = \int_0^t g(u)\,\mathrm{d}u\,. \tag{1}$$

The probability $p(t)$ also denotes the fraction of a heat quantity injected at time $t = 0$ arriving at the PTA within a time t. Then, if the heat flow introduced into the aquifer at the injection location is expressed as $I(t)$, the heat flowing through the PTA, $F_{PTA}(t)$, results from the convolution of the transfer function $g(t)$ with the introduced heat flow $I(t)$:

$$F_{PTA}(t) = \int_0^t g(u)I(t-u)\,\mathrm{d}u\,. \quad (2)$$

Subsequently, Eq. (2) is adopted for open- and closed-loop systems based on the following assumptions:

- A constant undisturbed background temperature T_a is considered.
- Heat transport is studied under steady-state hydraulic conditions and natural hydraulic fluctuations are assumed negligible. This also means that any external heat injection by a neighbouring system is assumed to have a negligible temporal influence on the flow regime. This is valid for closed-loop systems at any time when buoyancy and density effects can be ignored [26].
- The external heat injection can be described as constant input.

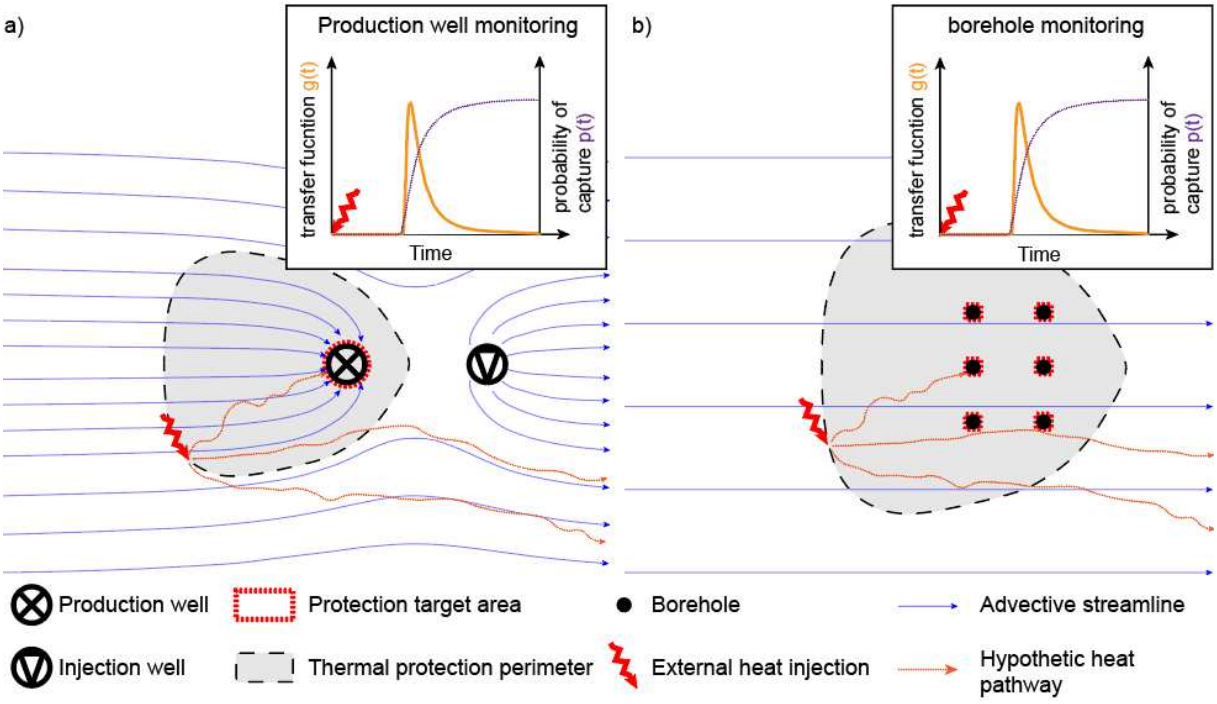

Figure 1: Illustration of protection target areas (PTA) of open-loop (a) and closed-loop (b) geothermal systems operating within a 2D model aquifer with a regional groundwater flow from the West to the East.

2.1 Open systems

In case of open-loop systems, the PTA is reduced to the location and surroundings of the production well (Fig. 1a). This is because only around the production well a capture zone can be delineated. Let us focus only on the fraction of heat produced additionally by a geothermal system as a consequence of interference. The heat flow $F_{PTA}^{Op}(t)$ abstracted from the aquifer by the production well due to the interference with the external heat injection at a given time is expressed as:

$$F_{PTA}^{Op}(t) = Q_p \cdot C_w \cdot (T_p(t) - T_a) \quad (3)$$

where Q_p is the pumping rate of the production well, C_w is the volumetric heat capacity of water, T_p is the groundwater temperature abstracted at the production well and T_a is the undisturbed temperature. Eqs. (2) and (3) can be combined as follows:

$$F_{PTA}^{Op}(t) = \int_0^t g(u)I(t-u)\,\mathrm{d}u = Q_p \cdot C_w \cdot (T_p(t) - T_a(t)) \quad (4)$$

As the external heat injection $I(t)$ is defined as a constant input, and considering Eq. (1), Eq. (4) can be rewritten:

$$I \cdot p(t) = Q_p \cdot C_w \cdot (T_p(t) - T_a) \quad (5)$$

This can be rearranged to express the temperature at the production well:

$$T_p(t) = T_a + \frac{I \cdot p(t)}{Q_p \cdot C_w} \quad (6)$$

For all time ranging from 0 to t, the condition to protect the production well of this open-loop system is expressed by

$$T_p(t) - T_a \leq \Delta T_{max} \quad (7)$$

Combining Eqs. (6) and (7), the thermal protection criteria is delineated by adhering to the following condition:

$$p(t) \leq \frac{\Delta T_{max} \cdot Q_p \cdot C_w}{I} \quad (8)$$

This criterion means that if the external heat injection I is located in an area where the heat probability of capture is low enough, the warming of abstracted groundwater at the production well of the open-loop system will be lower than ΔT_{max}.

2.2 Closed systems

In case of a closed-loop system, the PTA includes all BHEs of the installation (Fig. 1b). For each BHE, the heat power in place in groundwater of the associated area $F_{PTA}^{Cl}(t)$ is expressed as

$$F_{PTA}^{Cl}(t) = Q_D \cdot C_w \cdot (T_p(t) - T_a') \quad (9)$$

where Q_D is the fictive Darcy inflow calculated around the borehole of a diameter d:

$$Q_D = d \cdot v_a \cdot n \quad (10)$$

Here, T_p is the mean groundwater in the PTA and T_a' is the mean groundwater temperature in the PTA before any external injection of heat, and n represents the (effective) porosity. Considering that definition, $T_a' - T_a$ represents the mean thermal impact caused by the closed-loop system in the PTA. Following the same procedure as exposed for open-loop systems in Chap. 2.1, and replacing T_a by T_a' and Q_p by Q_D, we arrive at

$$p(t) \leq \frac{\Delta T_{max} \cdot Q_D \cdot C_w}{I} . \quad (11)$$

3 Quantifying thermal capture probabilities

Thermal capture probability refers to a given geothermal installation and is defined as the probability that the heat from any spatial point is transported to this installation. This yields a map of increasing thermal capture probability towards the installation. The concept of thermal capture probability is developed by exploiting the analogy with the description of an advective-dispersive solute transport problem [42, 43]. The mathematical technique to compute a probability field for a thermal quantity to reach a domain of interest assumes injection of a thermal pulse in the domain of interest, and it solves the heat transport equation considering a reverse flow. The probability field can then be calculated by integration of the heat signal moving in the backward direction. Because the thermal response of a pulse is the derivative function of the thermal response of a constant heat load, this problem can be equivalently solved by studying groundwater temperature disturbances in the backward direction caused by a constant thermal anomaly of, for instance, $\Delta T = 1\,K$ assigned at the location of the geothermal device. Consequently, any analytical and numerical models available for simulation of the thermal impact caused by a heat injection in groundwater in the forward direction of flow can be used to determine capture probabilities in the backward direction.

3.1 Open-loop systems

According to Stauffer et al. [7], there exists no exact analytical solution for simulating the thermal response of an aquifer that accounts for reinjection of water at a temperature different from the extracted water. However, to evaluate the zone of thermal influence or TAZ caused by an open-loop system, approximate solutions can be used. The applicability of semi-analytical techniques to predict the thermal plume around open-loop systems under uniform advective flow conditions was inspected by Pophillat et al. [37]. It was demonstrated that the planar advective heat transport model (PAHM), introduced by Domenico and Robbins [45] and modified by Hähnlein et al. [46], is appropriate for conditions with moderate groundwater flow velocity (1 m d^{-1}). The PAHM allows to compute downstream ($x > 0$) thermal anomalies caused by a warm/cold water injection located at the origin ($x = 0, y = 0$) in a two-dimensional (2D) model with groundwater flowing in the x-axis direction:

$$\Delta T(x,y,t) = \left(\frac{\Delta T_0}{4}\right) \mathrm{erfc}\left(\frac{\frac{C_m}{nC_w}x - v_a t}{2\sqrt{D_x R t}}\right) \left\{ \mathrm{erf}\left[\frac{y+\frac{Y}{2}}{2\sqrt{D_y \frac{x}{v_a}}}\right] - \mathrm{erf}\left[\frac{y-\frac{Y}{2}}{2\sqrt{D_y \frac{x}{v_a}}}\right] \right\} \tag{12}$$

with:

$$\Delta T_0 = \frac{F_0}{v_a n C_w Y} \tag{13}$$

$$F_0 = \frac{q_h}{b} \tag{14}$$

$$q_h = C_w \Delta T_{inj} Q_p \tag{15}$$

where F_0 is the energy injection per length of the aquifer (W m^{-1}), Y is the dimension of the source in the y-direction, and q_h is the injected heat power. The parameters D_x and D_y in Eq. (12) are the longitudinal and transversal hydrodynamic dispersion coefficients, respectively, and they are defined as follows:

$$D_{x/y} = \frac{\lambda_m}{nC_w} + \alpha_{L/T} v_a \tag{16}$$

The subscripts L and T refer to longitudinal and transversal direction with respect to the groundwater flow direction.

The source length Y is given by:

$$Y = \frac{Q_p}{b v_a n} \tag{17}$$

To calculate probability fields upstream of production wells of open-loop systems, Eq. (12) is rearranged considering $\Delta T_{inj} = 1$ K, and a reverse flow is assumed meaning that x becomes $-x$:

$$p_{op}(x,y,t) = \left(\frac{Q_p}{4 b v_a n Y}\right) \operatorname{erfc}\left(\frac{-\frac{C_m}{n C_w} x - v_a t}{2\sqrt{D_x R t}}\right) \left\{ \operatorname{erf}\left[\frac{y+\frac{Y}{2}}{2\sqrt{D_y \frac{-x}{v_a}}}\right] - \operatorname{erf}\left[\frac{y-\frac{Y}{2}}{2\sqrt{D_y \frac{-x}{v_a}}}\right] \right\} \tag{18}$$

This adapted model is implemented to quantify the probability of capture after an arbitrary period of 120 days (seasonal operation) around an open-loop system of 0.02 l s^{-1} m^{-1} (pumping rate by unit of aquifer thickness) operating in an aquifer with moderate groundwater flow velocity (1 m d^{-1}), and the result is illustrated in Figure 2a. Further details on model parameter values selected for this example are given in the appendix (Table A.1). The result shows that the thermal capture probability is close to 1 near the location of the production well and it decreases in the upstream direction. Since the adapted PAHM (Eq. 18) is only defined for the upstream, the thermal capture probability cannot be calculated downstream and thus here was set to 0 for x > 0. According to Fig. 2a, after 120 days, the probability of capture reaches about 10 % at 52 m upstream of the production well. This means that if a heat quantity is injected in the aquifer at this upstream location, 10 % of this energy is abstracted by the production well of the injection well before 120 days.

Assuming that abstracted groundwater should not be altered, for instance, by more than ΔT_{max}, Eq. (8) can be reformulated to calculate the maximal acceptable power that can be extracted from the upstream, MAP_{up}:

$$MAP_{up}(x,y) = \frac{\Delta T_{max} \cdot Q_p \cdot C_w}{p_{op}(x,y,t = 120 \text{ days})} \tag{19}$$

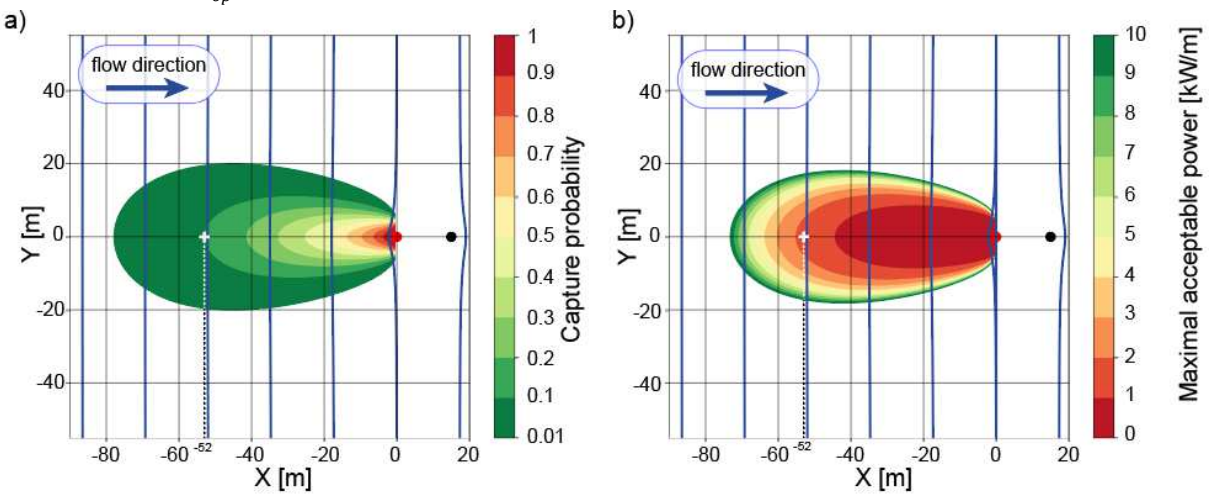

Figure 2: Illustration of (a) capture probabilities and (b) maximal acceptable power (assuming $\Delta T_{max} = 2$K) around an open-loop system operating in a 2D aquifer with a seepage velocity of 1 m per day. Piezometric isolines are represented by blue lines; the production well of the doublet is represented by a red dot and the injection well by a black dot.

The result is illustrated in Figure 2b. For example, it shows that 52 m upstream of the production well (white marks in Fig. 2), a new geothermal installation of 2 kW m^{-1} will alter the abstracted groundwater of the installation of interest by 2 K after 120 days. Because of the linear relationship between MAP_{up} and ΔT_{max}, (see Eq. (19)), the maximal acceptable power that would be exploitable considering another thermal threshold is easily calculable.

3.2 Closed-loop systems

Several analytical solutions are available to calculate the thermal response of an aquifer to operation of closed-loop geothermal systems [7]. In this study, the analytical model used to calculate capture probability around such systems is based on the moving infinite line source theory initially proposed by Carslaw and Jaeger [47]. This semi-analytical model allows for the calculation the thermal response of a line source of infinite length along the vertical direction with a continuous heat flow rate q_{tb} per unit length of the BHE in a uniform advective-dispersive flow system. According to Stauffer et al. [7] the moving infinite line source model considering dispersion (MILD) reads

$$\Delta T(x,y,t) = \frac{q_{th}}{4\pi C_m \sqrt{D_{t,L} D_{t,T}}} \exp\left[\frac{u_t x}{2D_{t,L}}\right] \times \int_{\frac{x^2}{4D_{t,L}t}+\frac{y^2}{4D_{t,T}t}}^{\infty} \exp\left[-\Psi - \left(\frac{x^2}{D_{t,L}} + \frac{y^2}{D_{t,T}}\right)\frac{u_t^2}{16 D_{t,L}\Psi}\right]\frac{\mathrm{d}\Psi}{\Psi} \tag{20}$$

with:

$$u_t = \frac{C_w n}{C_m} v_a \tag{21}$$

$$D_{t,L/T} = \frac{\lambda_m}{C_w} + \alpha_{L/T} u_t \tag{22}$$

To calculate probability fields upstream of heat extracting closed-loop systems, Eq. (20) is rearranged. For this, again reverse flow is described by replacing x with $-x$. In addition to that, q_{th} is expressed as the power per unit length needed to reheat by 1 K the virtual Darcy flow rate (per unit length) crossing the BHE location:

$$q_{th} = KidC_w \tag{23}$$

where K is the hydraulic conductivity, i is the hydraulic gradient, and d represents the borehole diameter. This yields the probability field around a borehole located at the origin ($x = 0, y = 0$):

$$p_{BHE}^{k}(x,y,t) = \frac{KidC_w}{4\pi C_m \sqrt{D_{t,L} D_{t,T}}} \exp\left[\frac{-u_t x}{2D_{t,L}}\right] \times \int_{\frac{x^2}{4D_{t,L}t}+\frac{y^2}{4D_{t,T}t}}^{\infty} \exp\left[-\Psi - \left(\frac{x^2}{D_{t,L}} + \frac{y^2}{D_{t,T}}\right)\frac{u_t^2}{16 D_{t,L}\Psi}\right]\frac{\mathrm{d}\Psi}{\Psi} \tag{24}$$

Since the probability that a thermal alteration will reach the installation is equal to the sum of probabilities to reach individual BHEs, we arrive at:

$$p_{cl}(x,y,t) = \sum_k p_{BHE}^{k}(x,y,t) \tag{25}$$

For demonstration, similar to the open-loop example above, this adapted MILD model is employed to quantify the probability of capture after 120 days (seasonal operation) around different BHE configurations with a diameter d of 1 m operating in an aquifer with moderate groundwater flow velocity (1 m d^{-1}). Again, further details on model settings can be found in the appendix (Table A.1). For a single BHE, the result is illustrated in Figure 3a,b, and it shows that thermal capture probabilities

near the installation are much lower than for an open-loop system (Figure 2a). For example, 10 m upstream the BHE, the probability of capture is within a range of 10% - 20% in contrast to 60% - 70% in the open-loop case. This is explained by the fact that in case of open-loop systems, groundwater flow locally converges towards the production well, which does not happen for closed-loop systems.

Assuming, equivalent to the example for the open-loop system above, that groundwater should not be altered by more than ΔT_{max} at BHEs locations, Eq. (10) is reformulated to calculate the maximal acceptable power MAP_{BHE}^{k} that can be exploited around each BHE (k):

$$MAP_{BHE}^{k}(x,y) = \frac{\Delta T_{max} \cdot Q_D \cdot C_w}{p_{BHE}^{k}(x,y,t = 120\ \text{days})} \tag{26}$$

Then, to protect all BHE within the PTA from a temperature alteration, the maximal acceptable power MAP_{cl} that can be exploited around the installation reads:

$$MAP_{cl}(x,y,t) = \min_{k}(MAP_{BHE}^{k}(x,y,t)) \tag{27}$$

The result is illustrated in Figure 3b for a single BHE, assuming $\Delta T_{max} = 2\text{K}$. It shows that for example 60 m upstream of the BHE, a hypothetical new geothermal installation of 3 kW m^{-1} alters the temperature in the vicinity of the installation of interest by 2 K after 120 days. The probability of capture and the maximal acceptable power that can be exploited depends on the configuration, when multiple BHEs are implemented. This is illustrated in different examples with six BHEs in Fig. 3. If the BHEs are aligned perpendicularly to the groundwater flow direction (Fig. 3c,d), the capture zone becomes wider, whereas the zone is elongated when arranged in line with the groundwater flow direction (Fig. 3e,f). The intermediate case with a common lattice arrangement is depicted in Fig. 3g,h.

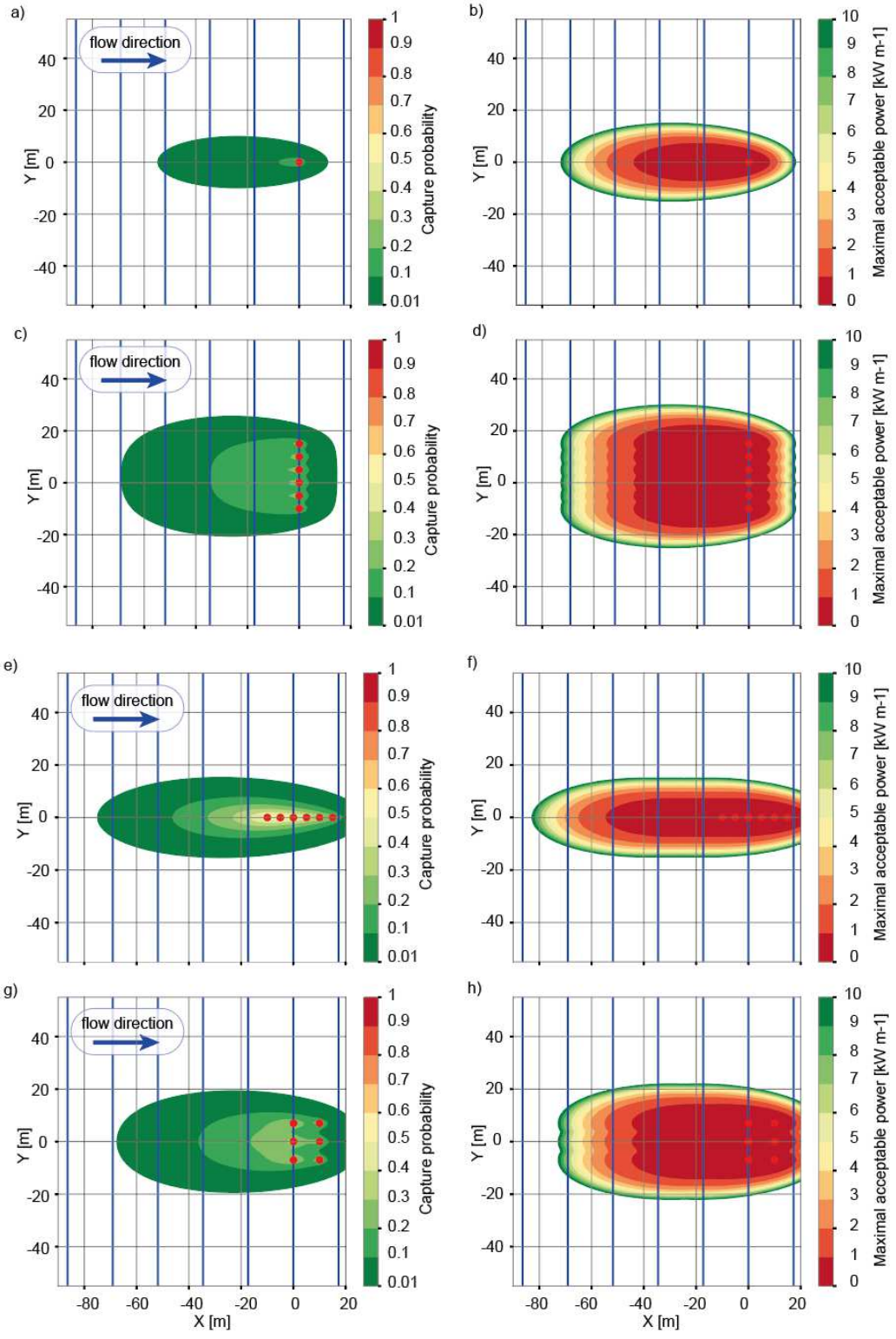

Figure 3: Illustration of capture probabilities and maximal acceptable power after 120 days around different BHEs configurations operating in a 2D aquifer with a seepage velocity of 1 m per day (assuming $\Delta T_{max} = 2$K). Piezometric isolines are represented by blue lines and BHE are represented by red dots. (a, b) single BHE, (c, d) field of six BHEs perpendicular to the groundwater flow direction, (e,f) field of six BHEs in line with the groundwater flow direction and (g, h) field of six BHEs organized as a rectangular grid.

4 Applications

4.1 Multiple open geothermal installations in the city of Lyon (France)

The selected studied area of 4 km² is located in Lyon (France) (45.75°N/4.85°E). The hydrogeologic characteristics of this sector were previously investigated [48, 49]. In this urban area, the groundwater flows under unconfined conditions with a regional hydraulic gradient of 0.2% through a 25 m thick fluvial deposit with an effective porosity of 20% and a hydraulic conductivity of 0.001 m s^{-1}. In this sector, piezometric levels are influenced by underground structures and particularly by four underground car parks equipped with draining and reinjection systems. Open-loop systems in Lyon have been investigated since 2012 by the French Geological Survey [50]. In our studied area, six open geothermal installations are reported with maximal pumping rates ranging from 1.5 to 16.5 l s^{-1} and inducing a temperature difference ranging from 5 to 12 K. These installations are only used for temporal cooling in summer.

To prevent long-term interferences with new installations, probabilities of capture are calculated around these installations using the PAHM considering five years of operation at the maximal power (Fig. 4a). Then, the maximal acceptable power for any new installation to avoid interference is obtained by the four following steps:

- A background maximal acceptable power (BMAP) is calculated. This considers an acceptable drawdown $\Delta(r,t)$ of 1 m, at a distance of 1 m from a production well, and after one week of operation. First, the Theis equation (Eq. 28) is employed to determine the maximal pumping rate Q:

$$\Delta(r,t) = \frac{Q}{4\pi \cdot K \cdot e} W(u) \text{ with } u = \frac{r^2 \cdot S}{4 \cdot K \cdot e \cdot t} \text{ and } W(u) = \int_u^{+\infty} \frac{e^{-v}}{v} \mathrm{d}v \quad (28)$$

  This is used to determine BMAP considering a standard temperature difference of ΔT_s =10 K between the production and the injection well, a volumetric heat capacity of water of C_w = 4.18 10^6 J m^{-3} s^{-1}; this gives approximately BMAP = 1000 kW:

$$\mathrm{BMAP}(x,y) = Q \cdot C_w \cdot (T_0 - T_{inj}) \quad (29)$$

- The second step considers thermal capture probabilities to determine the maximal acceptable power upstream of a given installation *k*, MAP_{up}^{k} using Eq. (19). This equation is applied assuming that $\Delta T_{max} = 2K$ (the maximal temperature alteration allowed at the production well), and $p(t = 5\,\text{years})$, which is the probability of a thermal change to reach the production well within 5 years of operation.
- Because the PAHM is not defined downstream of production wells, a third step is implemented to avoid an important gap of maximal acceptable power between the area at *x'* > 0 and the area at *x'* < 0 (where (±x') represents the regional direction of flow). This third step is calculating the maximal acceptable power downstream from an installation *k* (MAP_{dw}^{k}). This calculation is based on the non-recycling criteria of open-loop systems formulated by Lippmann and Tsang [6]. Accordingly, production and injection wells of a doublet should be separated by a distance *L* to avoid thermal recycling:

$$L \geq \frac{2 \cdot Q_k}{K \cdot i \cdot b \cdot \pi} \quad (30)$$

  Given the standard temperature difference ΔT_s = 10 K, we get

$$MAP_{dw}^{k}(x,y) = \frac{L \cdot K \cdot i \cdot b \cdot \pi}{2 \cdot \Delta T_s} \quad (31)$$

where L represents the distance between the production well and the point location (x, y).

- The three previous steps are then applied on a regular grid with cells of 2 m × 2 m by looping over the six production wells and over the nodes of the grid. The result of this process is illustrated in Fig. 4b. The final expression of the maximal acceptable power (MAP) is given by

$$MAP(x,y) = \min_k(\mathrm{BMAP}(x,y), MAP_{dw}^k(x,y), MAP_{up}^k(x,y)) \quad (32)$$

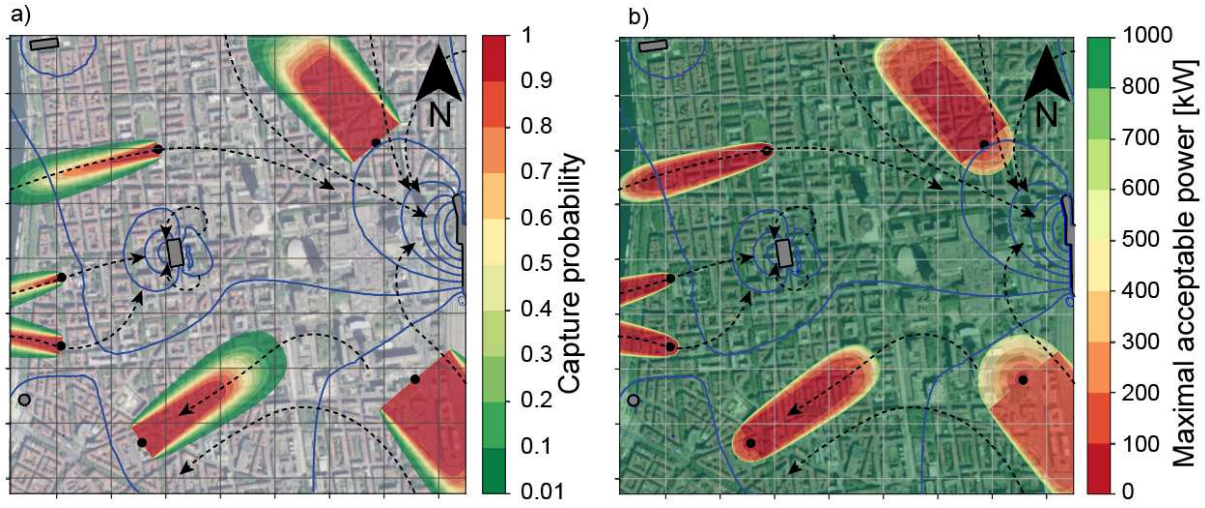

Figure 4: a) Capture probabilities around multiple installations in Lyon (France). Piezometric isolines (from Attard et al. [48]) are represented in blue (0.5 m step) and local groundwater flow direction is indicated by black doted arrows. b) Maximal acceptable power for a new installation. The grid cells are 200 m × 200 m.

4.2 Delineation of thermal protection perimeters

Figure 4 shows that the results given by local application of analytical solutions strongly depend on the local groundwater flow direction. Furthermore, urban underground characteristics (e.g. underground structures, heterogeneous recharge) can compromise the spatial representativeness of results offered by analytical solutions. In that case, the flexibility of numerical modelling can help to provide a better accuracy of flow systems in urban area by a more comprehensive integration of underground complexity.

Here, a numerical simulation was performed to determine the maximal acceptable power that can be exploited around an open-loop installation located in an area of Lyon where groundwater flow is disturbed by several impervious underground constructions. The 2D modelling procedure consists of solving transient heat transport and flow equations for the entire studied area. Groundwater flow and heat transport are simulated using the finite element based software FEFLOW [51].

The first step of the modelling process consists in simulating steady groundwater flows over the area of interest. The modelling configuration used is illustrated in Fig. 5a and the parametrization is detailed in the appendix (Table A.1). Both abstraction (red dot) and injection (black dot) wells are represented by the numerical model. The doublet has an average annual pumping rate of Q_P = 4.5 l s^{-1} which is assigned as a well boundary condition at the abstraction and injection locations. Impervious underground constructions are delineated by no-flux boundaries. The size of the elements ranges from several centimetres near underground constructions and wells to about a meter near to the domain

boundaries. For further details on the model sensitivity and calibration, readers are referred to previous papers focusing on the construction of this numerical model [48, 49].

The second step consists in reversing the flow direction over the studied area. Flow reversion can be done by inverting the sign of every flow boundary conditions values. In that case, water particles move from downstream to upstream; inlet becomes outlet and vice versa. Finally, the third step consists in quantifying the thermal probability of capture around the production well in the steady reverse flow field. A heat source boundary condition (19 kW) is assigned to the well location in the model. This heat source represents the power needed to alter abstracted groundwater by ΔT = 1 K. Then, the divergence form of the heat transport equation is solved assuming a reverse steady flow situation. The transient heat transport simulation time is set 5 years. The heat transport is assumed to be stabilized after that time which is in line with previous heat transport simulations made with this numerical model [49].

The resulting capture probability and the maximal acceptable power that can be exploited in the vicinity of the installation are illustrated in Figure 5. The simulation results show that the shape of capture probability fringes is highly influenced by underground impervious structures. Figure 5b also reveals that around the production well of the receptor doublet, groundwater flow is influenced by the existing injection well of another geothermal installation located 330 m in the upstream. This installation operates with a maximal injection flow rate of 6.8 l s^{-1}. However, the probability of heat capture at the doublet before 5 years is lower than 1%. This means that the injection well has no significant influence on the temperature of abstracted groundwater by the doublet.

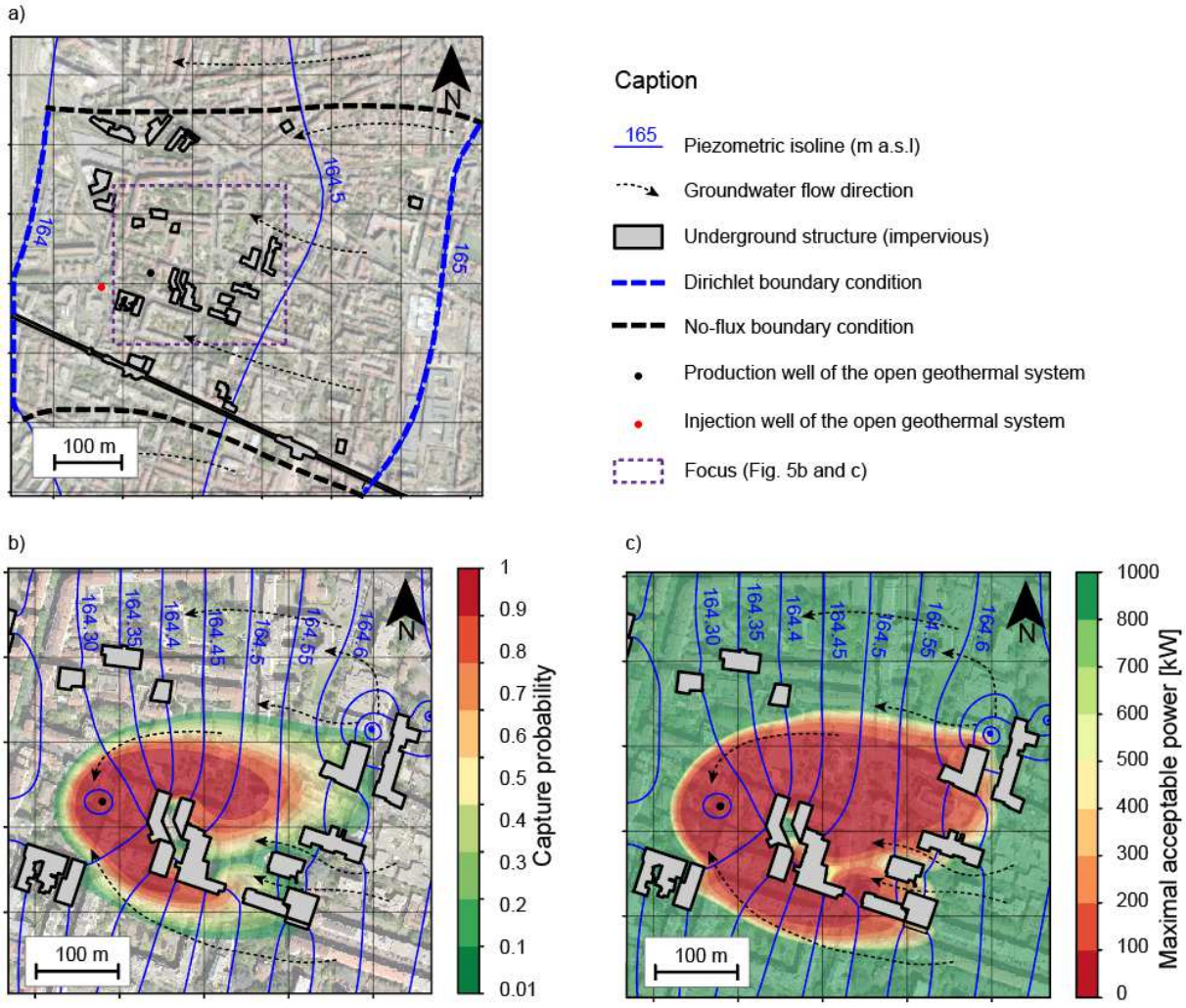

Figure 5 a) Study site in Lyon with boundary conditions and flow configuration; b) thermal capture probabilities around the geothermal installation (numerical approach); c) maximal acceptable power in the vicinity of the geothermal doublet installation.

Discussion and conclusions

The presented methodology is intended to prevent thermal interference between both open- and closed-loop systems. To our knowledge, this is the first generalized methodology that includes both geothermal variants and allows the mapping of a technical geothermal potential accounting for interference. It relies on the theory of transfer functions in hydrogeology which was suggested to heat transport problems by Milnes and Perrochet [44] to assess the impact of thermal feedback and recycling within single geothermal well doublets. Here, the application of this theory was extended to the calculation of the probability of thermal capture around neighbouring installations. It allows for the understanding of where the extracted heat is coming from and what the heat contribution of various neighbouring sources would be. By linking a thermal threshold with capture probability, this methodology allows us to continuously and spatially quantify the compatibility between existing and planned new geothermal installations. This is not feasible by mapping thermal plumes caused by existing installations as done in common practice.

Two analytical models, PAHM and MILD are adapted to calculate thermal capture probabilities around respectively open- and closed-loop geothermal systems. It should be noted that the presented methodology can be applied using any other analytical solutions depending on the aim of a study,

scale (e.g. 2D, 3D) and the hydrogeological context. For example, in case of open-loop systems, Pophillat et al. [37] showed that the radial heat transport model by Guimerà et al. [52] is suitable under slow groundwater velocities (~0 m d^{-1}). The linear heat transport model by Kinzelbach [53] addresses high groundwater velocities (~10 m d^{-1}). In case of closed-loop systems, analytical solutions based on the moving finite line source theory [36, 54, 55] are available, and recent developments enable for the determination of the thermal response of closed-loop systems in three dimension and also resolve in detail the heat between underground and atmosphere [56-58].

The implementation of the PAHM illustrates how capture probabilities can help to manage multiple geothermal installations at the scale of an urbanized area of a few square kilometres. However, because the calculation of capture probabilities relies on an assumption of steady-state hydraulic conditions, the interpretation of the maximal power that can be exploited around the installation is valid only when the hydraulic disturbance caused by the planned new installation is marginal. In case of significant change of the groundwater flow regime, this needs to be accounted for; for example, by using numerical simulation prediction and revision of the original piezometric map.

In addition, it is obvious that the results given by this approach have a strong dependency on local groundwater flow directions. Consequently, the technical geothermal potential maps that can be obtained by this approach need to be revised when the groundwater regime changes. This is the case, for example, when a (massive) new underground structure is built.

Finally, because the application of this methodology can have consequences on regulatory geothermal licensing, the uncertainty in the delineation of management areas around installations has to be fully addressed. In this regard, Chow et al. [38] explained that the approach based on the calculation of capture probabilities is adapted to the representation of local scale uncertainties, especially because this calculation builds upon the macrodispersion theory. This makes the assessment of thermal dispersivity coefficients particularly crucial. However, for the delineation of protection perimeters around water supply wells, they showed that large scale uncertainties can be addressed by modeling and comparing a few numbers of realistic scenarios.

Acknowledgements

This work was supported by the French Ministry of Ecological and Solidarity Transition. We also thank the German Research Foundation for support through the project BA2850/3-1.

Appendix

Table A.1 : Parameter values for the analytical and numerical models

Model settings	Analytical model PAHM (Section 3.2)	Analytical model MILS (Section 3.2)	Numerical model (Section 4.2)
Simulation time	120 days		5 years
b : Aquifer thickness (m)	2D - horizontal		25
n : Effective porosity (%)	20		

K: Hydraulic conductivity (m s^{-1})	10^{-3}	
i: Hydraulic gradient[a]	2.3×10^{-3}	-
α_L: Londitudinal dispersivity (m)	5	
α_T: Transversal dispersivity (m)	0.5	
c_w : Volumetric heat capacity of water (MJ m^{-3} K^{-1})	4.2	
c_s: Volumetric heat capacity of solid (MJ m^{-3} K^{-1})	2.52	
λ_w: Thermal conductivity of fluid (J m^{-1} s^{-1} K^{-1})	0.65	
λ_s: Thermal conductivity of solid (J m^{-1} s^{-1} K^{-1})	3	
λ_m: Thermal conductivity of the porous media[a] (J m^{-1} s^{-1} K^{-1})	2.24	

413 [a] This parameter was assigned only for the analytical scenarios.

References

[1] S.J. Rees, An introduction to ground-source heat pump technology, Advances in Ground-Source Heat Pump Systems, Elsevier2016, pp. 1-25.

[2] N. Daemi, M.M. Krol, Impact of building thermal load on the developed thermal plumes of a multi-borehole GSHP system in different canadian climates, Renewable Energy 134 (2019) 550-557.

[3] P. Bayer, G. Attard, P. Blum, K. Menberg, The geothermal potential of cities, Renewable and Sustainable Energy Reviews 106 (2019) 17-30.

[4] L. Alberti, M. Antelmi, A. Angelotti, G. Formentin, Geothermal heat pumps for sustainable farm climatization and field irrigation, Agricultural Water Management 195 (2018) 187-200.

[5] M. Le Lous, F. Larroque, A. Dupuy, A. Moignard, P.-C. Damy, Performance of an open-loop well-doublet scheme located in a deep aquitard–aquifer system: Insights from a synthetic coupled heat and flow model, Geothermics 74 (2018) 74-91.

[6] M.J. Lippmann, C.F. Tsang, Ground-Water Use for Cooling: Associated Aquifer Temperature Changes, Groundwater 18(5) (1980) 452-458.

[7] F. Stauffer, P. Bayer, P. Blum, N.M. Giraldo, W. Kinzelbach, Thermal use of shallow groundwater, CRC Press2013.

[8] S. Haehnlein, P. Bayer, P. Blum, International legal status of the use of shallow geothermal energy, Renewable and Sustainable Energy Reviews 14(9) (2010) 2611-2625.

[9] S. Hähnlein, P. Bayer, G. Ferguson, P. Blum, Sustainability and policy for the thermal use of shallow geothermal energy, Energy Policy 59 (2013) 914-925.

[10] G. Ferguson, Unfinished business in geothermal energy, GroundWater 47(2) (2009) 167-167.

[11] T. Vienken, S. Schelenz, K. Rink, P. Dietrich, Sustainable intensive thermal use of the shallow subsurface—a critical view on the status quo, Groundwater 53(3) (2015) 356-361.

[12] S.M. Maya, A. García-Gil, E.G. Schneider, M.M. Moreno, J. Epting, E. Vázquez-Suñé, M.Á. Marazuela, J.Á. Sánchez-Navarro, An upscaling procedure for the optimal implementation of open-loop geothermal energy systems into hydrogeological models, Journal of hydrology 563 (2018) 155-166.

[13] P.L. Younger, Ground-coupled heating-cooling systems in urban areas: how sustainable are they?, Bulletin of Science, Technology & Society 28(2) (2008) 174-182.

[14] J. Kim, Y. Nam, A numerical study on system performance of groundwater heat pumps, Energies 9(1) (2016) 4.

[15] S. Miglani, K. Orehounig, J. Carmeliet, A methodology to calculate long-term shallow geothermal energy potential for an urban neighbourhood, Energy and Buildings 159 (2018) 462-473.

[16] Y.L.E. Law, S.B. Dworkin, Characterization of the effects of borehole configuration and interference with long term ground temperature modelling of ground source heat pumps, Applied energy 179 (2016) 1032-1047.

[17] C. Tissen, K. Menberg, P. Bayer, P. Blum, Meeting the demand: geothermal heat supply rates for an urban quarter in Germany, Geothermal Energy 7(1) (2019) 9.

[18] H. Brielmann, T. Lueders, K. Schreglmann, F. Ferraro, M. Avramov, V. Hammerl, P. Blum, P. Bayer, C. Griebler, Oberflächennahe Geothermie und ihre potenziellen Auswirkungen auf Grundwasserökosysteme, Grundwasser 16(2) (2011) 77.

[19] C. Griebler, H. Brielmann, C.M. Haberer, S. Kaschuba, C. Kellermann, C. Stumpp, F. Hegler, D. Kuntz, S. Walker-Hertkorn, T. Lueders, Potential impacts of geothermal energy use and storage of heat on groundwater quality, biodiversity, and ecosystem processes, Environmental Earth Sciences 75(20) (2016) 1391.

[20] M. Alcaraz, L. Vives, E. Vázquez-Suñé, The TI-GER method: A graphical alternative to support the design and management of shallow geothermal energy exploitations at the metropolitan scale, Renewable Energy 109 (2017) 213-221.

[21] J.A. Rivera, P. Blum, P. Bayer, Increased ground temperatures in urban areas: Estimation of the technical geothermal potential, Renewable energy 103 (2017) 388-400.

[22] A. García-Gil, S.M. Maya, E.G. Schneider, M.M. Moreno, E. Vázquez-Suñé, M.Á. Marazuela, J.M. Lázaro, J.Á. Sánchez-Navarro, Sustainability indicator for the prevention of potential thermal interferences between groundwater heat pump systems in urban aquifers, Renewable Energy 134 (2019) 14-24.

[23] M.H. Mueller, P. Huggenberger, J. Epting, Combining monitoring and modelling tools as a basis for city-scale concepts for a sustainable thermal management of urban groundwater resources, Science of The Total Environment 627 (2018) 1121-1136.
[24] J. Epting, M.H. Müller, D. Genske, P. Huggenberger, Relating groundwater heat-potential to city-scale heat-demand: A theoretical consideration for urban groundwater resource management, Applied energy 228 (2018) 1499-1505.
[25] F. Händel, R. Liedl, J. Fank, G. Rock, Regional modeling of geothermal energy systems in shallow aquifers: the Leibnitzer Feld case study (Austria), Environmental earth sciences 70(8) (2013) 3433-3446.
[26] J. Hecht-Méndez, N. Molina-Giraldo, P. Blum, P. Bayer, Evaluating MT3DMS for heat transport simulation of closed geothermal systems, Groundwater 48(5) (2010) 741-756.
[27] M. Beck, P. Bayer, M. de Paly, J. Hecht-Méndez, A. Zell, Geometric arrangement and operation mode adjustment in low-enthalpy geothermal borehole fields for heating, Energy 49 (2013) 434-443.
[28] D. Marcotte, P. Pasquier, Fast fluid and ground temperature computation for geothermal ground-loop heat exchanger systems, Geothermics 37(6) (2008) 651-665.
[29] H.J. Witte, A Novel Tool for Assessing Negative Temperature Interactions between Neighbouring Borehole Heat Exchanger Systems, 14th international conference on energy storafge, 2018.
[30] S. Erol, B. François, Multilayer analytical model for vertical ground heat exchanger with groundwater flow, Geothermics 71 (2018) 294-305.
[31] B. Piga, A. Casasso, F. Pace, A. Godio, R. Sethi, Thermal impact assessment of groundwater heat pumps (GWHPs): Rigorous vs. simplified models, Energies 10(9) (2017) 1385.
[32] A. García-Gil, E. Vázquez-Suñe, E.G. Schneider, J.Á. Sánchez-Navarro, J. Mateo-Lázaro, Relaxation factor for geothermal use development–Criteria for a more fair and sustainable geothermal use of shallow energy resources, Geothermics 56 (2015) 128-137.
[33] X. Zhou, Q. Gao, X. Chen, M. Yu, X. Zhao, Numerically simulating the thermal behaviors in groundwater wells of groundwater heat pump, Energy 61 (2013) 240-247.
[34] A. Herbert, S. Arthur, G. Chillingworth, Thermal modelling of large scale exploitation of ground source energy in urban aquifers as a resource management tool, Applied energy 109 (2013) 94-103.
[35] S.L. Russo, L. Gnavi, E. Roccia, G. Taddia, V. Verda, Groundwater Heat Pump (GWHP) system modeling and Thermal Affected Zone (TAZ) prediction reliability: Influence of temporal variations in flow discharge and injection temperature, Geothermics 51 (2014) 103-112.
[36] N. Molina-Giraldo, P. Blum, K. Zhu, P. Bayer, Z. Fang, A moving finite line source model to simulate borehole heat exchangers with groundwater advection, International Journal of Thermal Sciences 50(12) (2011) 2506-2513.
[37] W. Pophillat, G. Attard, P. Bayer, J. Hecht-Méndez, P. Blum, Analytical solutions for predicting thermal plumes of groundwater heat pump systems, Renewable energy (2018).
[38] R. Chow, M.E. Frind, E.O. Frind, J.P. Jones, M.R. Sousa, D.L. Rudolph, J.W. Molson, W. Nowak, Delineating baseflow contribution areas for streams–A model and methods comparison, Journal of contaminant hydrology 195 (2016) 11-22.
[39] J. Molson, E. Frind, On the use of mean groundwater age, life expectancy and capture probability for defining aquifer vulnerability and time-of-travel zones for source water protection, Journal of contaminant hydrology 127(1-4) (2012) 76-87.
[40] C. Turnadge, B.D. Smerdon, A review of methods for modelling environmental tracers in groundwater: advantages of tracer concentration simulation, Journal of Hydrology 519 (2014) 3674-3689.
[41] G.A. Kazemi, J.H. Lehr, P. Perrochet, Groundwater age, John Wiley & Sons2006.
[42] F. Cornaton, P. Perrochet, Groundwater age, life expectancy and transit time distributions in advective–dispersive systems: 1. Generalized reservoir theory, Advances in Water Resources 29(9) (2006) 1267-1291.
[43] F. Cornaton, P. Perrochet, Groundwater age, life expectancy and transit time distributions in advective–dispersive systems; 2. Reservoir theory for sub-drainage basins, Advances in water resources 29(9) (2006) 1292-1305.

[44] E. Milnes, P. Perrochet, Assessing the impact of thermal feedback and recycling in open-loop groundwater heat pump (GWHP) systems: a complementary design tool, Hydrogeology journal 21(2) (2013) 505-514.
[45] P. Domenico, G. Robbins, A new method of contaminant plume analysis, Groundwater 23(4) (1985) 476-485.
[46] S. Hähnlein, N. Molina-Giraldo, P. Blum, P. Bayer, P. Grathwohl, Ausbreitung von Kältefahnen im Grundwasser bei Erdwärmesonden, Grundwasser 15(2) (2010) 123-133.
[47] H.S. Carslaw, J.C. Jaeger, Conduction of heat in solids, Oxford: Clarendon Press, 1959, 2nd ed. (1959).
[48] G. Attard, Y. Rossier, T. Winiarski, L. Cuvillier, L. Eisenlohr, Deterministic modelling of the cumulative impacts of underground structures on urban groundwater flow and the definition of a potential state of urban groundwater flow: example of Lyon, France, Hydrogeology journal 24(5) (2016) 1213-1229.
[49] G. Attard, Y. Rossier, T. Winiarski, L. Eisenlohr, Deterministic modeling of the impact of underground structures on urban groundwater temperature, Science of the Total Environment 572 (2016) 986-994.
[50] P. Durst, F. Garnier, M. Parmentier, D. Bezelgues Courtade, I. Ignatiadis, S. Orofino, F. Levillon, ImPAC Lyon: Évaluation de l'impact environnemental du aux modifications thermiques induites par les PAC sur les aquifères superficiels-Année 2. Rapport final, BRGM RP-60786-FR, 2012.
[51] H.-J.G. Diersch, FEFLOW: finite element modeling of flow, mass and heat transport in porous and fractured media, Springer Science & Business Media2013.
[52] J. Guimerà, F. Ortuño, E. Ruiz, A. Delos, A. Pérez-Paricio, Influence of ground-source heat pumps on groundwater, Actas del congreso European Geothemal Congres 2007 (Unterhaching, Alemania, 30 de mayo y 1 de junio de 2007), 2007.
[53] W. Kinzelbach, Numerische Methoden zur Modellierung des Transports von Schadstoffen im Grundwasser, Oldenbourg1987.
[54] M. Verdoya, C. Pacetti, P. Chiozzi, C. Invernizzi, Thermophysical parameters from laboratory measurements and in-situ tests in borehole heat exchangers, Applied Thermal Engineering 144 (2018) 711-720.
[55] M. Tye-Gingras, L. Gosselin, Generic ground response functions for ground exchangers in the presence of groundwater flow, Renewable energy 72 (2014) 354-366.
[56] J.A. Rivera, P. Blum, P. Bayer, Analytical simulation of groundwater flow and land surface effects on thermal plumes of borehole heat exchangers, Applied Energy 146 (2015) 421-433.
[57] J.A. Rivera, P. Blum, P. Bayer, A finite line source model with Cauchy-type top boundary conditions for simulating near surface effects on borehole heat exchangers, Energy 98 (2016) 50-63.
[58] J.A. Rivera, P. Blum, P. Bayer, Influence of spatially variable ground heat flux on closed-loop geothermal systems: Line source model with nonhomogeneous Cauchy-type top boundary conditions, Applied energy 180 (2016) 572-585.